



Rescue of synaptosomal glutamate release defects in tau transgenic mice by the tau aggregation inhibitor hydromethylthionine

Anna L. Cranston^a, Igor Kraev^b, Mike G. Stewart^{b,1}, David Horsley^a, Renato X. Santos^a, Lianne Robinson^a, Eline Dreesen^a, Paul Armstrong^a, Soumya Palliyil^c, Charles R. Harrington^{a,d}, Claude M. Wischik^{a,d}, Gernot Riedel^{a,*}

^a School of Medicine, Medical Sciences & Nutrition, University of Aberdeen, Foresterhill AB25 2ZD, UK

^b School of Life, Health and Chemical Sciences, The Open University, Milton Keynes MK7 6AA, UK

^c Scottish Biologics Facility, University of Aberdeen, Foresterhill AB25 2ZP, UK

^d TauRx Therapeutics Ltd, 395 King Street, Aberdeen, AB24 5RP, UK

ARTICLE INFO

Keywords:

Alzheimer's disease, glutamate
Frontotemporal lobar degeneration
Synaptosomes
Hydromethylthionine

ABSTRACT

Glutamatergic neurotransmission, important for learning and memory, is disrupted in different ways in patients with Alzheimer's disease (AD) and frontotemporal dementia (FTD) tauopathies. We have previously reported that two tau transgenic mouse models, L1 and L66, produce different phenotypes resembling AD and FTD, respectively. The AD-like L1 model expresses the truncated core aggregation domain of the AD paired helical filament (PHF) form of tau (tau296–390) whereas the FTD-like L66 model expresses full-length tau carrying two mutations at P301S/G335D. We have used synaptosomes isolated from these mice to investigate K⁺-evoked glutamate release and, if abnormal, to determine responsiveness to hydromethylthionine, a tau aggregation inhibitor previously shown to reduce tau pathology in these models. We report that the transgenes in these two mouse lines cause opposite abnormalities in glutamate release. Over-expression of the core tau unit in L1 produces a significant reduction in glutamate release and a loss of Ca²⁺-dependency compared with wild-type control mice. Full-length mutant tau produces an increase in glutamate release that retains normal Ca²⁺-dependency. Chronic pre-treatment with hydromethylthionine normalises both reduced (L1) and excessive glutamate (L66) and restores normal Ca²⁺-dependency in L1 mice. This implies that both patterns of impairment are the result of tau aggregation, but that the direction and Ca²⁺-dependency of the abnormality is determined by expression of the disease-specific transgene. Our results lead to the conclusion that the tauopathies need not be considered a single entity in terms of the downstream effects of pathological aggregation of tau protein. In this case, directionally opposite abnormalities in glutamate release resulting from different types of tau aggregation in the two mouse models can be corrected by hydromethylthionine. This may help to explain the activity of hydromethylthionine on cognitive decline and brain atrophy in both AD and behavioural-variant FTD.

1. Introduction

The majority of cases of Alzheimer's disease (AD) and some members of the frontotemporal lobar degeneration (FTLD) syndromes are characterised by pathological aggregation of tau protein that have come to be known collectively as tauopathies [1–3]. Of the FTLD syndromes, the most prevalent is behavioural variant frontotemporal dementia (bvFTD; [4]). The tau pathology in AD affects primarily the pyramidal cells of layers III and V of the cortex [5] and there is a significant loss of

glutamatergic pyramidal hippocampal neurons in the CA1 and CA3 regions [6]. In FTD, pathological tau accumulates primarily in GABA-ergic interneurons and astrocytes in molecular layers II and VI [7,8], where astrocytic pathology predominates [9] and is closely linked to disease severity [10]. There are also clinically important neurochemical differences between AD and FTD. There is no cholinergic deficit in FTD [11] whereas this is an important feature of AD [12]. There is no benefit from treatment with either cholinesterase inhibitors [13] or memantine [14] in FTD, whereas both classes of drugs are licensed for treatment of AD

* Corresponding author at: University of Aberdeen, Institute of Medical Sciences, Foresterhill, Aberdeen, Scotland AB25 2ZD, UK.

E-mail address: g.riedel@abdn.ac.uk (G. Riedel).

¹ Dedicated to the memory of Michael G. Stewart

<https://doi.org/10.1016/j.cellsig.2024.111269>

Received 26 February 2024; Received in revised form 13 June 2024; Accepted 20 June 2024

Available online 21 June 2024

0898-6568/Crown Copyright © 2024 Published by Elsevier Inc. This is an open access article under the CC BY license (<http://creativecommons.org/licenses/by/4.0/>).

[15].

Despite the central role of glutamatergic synapses in learning and memory [16], and the importance of vesicular glutamate exocytosis as a critical underpinning of memory formation and synaptic plasticity [17–19], the relationship between tau pathology and glutamate function in AD and FTD remains unclear. A decrease in post-synaptic metabotropic glutamate receptor 5 (mGlu5) has been reported in the brain of bvFTD patients [20] suggesting that glutamate-mediated excitotoxicity plays a role in the pathogenesis of bvFTD. This may also explain the reduced expression of both ionic GluRs (AMPA and NMDA types) in frontal and temporal cortices of FTD patients [21] as a mechanism of homeostatic adjustment to chronically elevated glutamate levels. Chronic elevation of synaptic glutamate levels poses a severe challenge to the tripartite synapse (for review, see [22]) since the main clearance pathway is through Na^+ -dependent astrocyte specific glutamate transporters, GLT-1 and GLAST [23,24]. Furthermore, disease severity in bvFTD is closely linked to the extent of pathology in astrocytes [10], which are responsible for 90% of the clearance of glutamate from synapses [25,26].

Although studies in bvFTD, and FTD more generally, are consistent with the idea of chronic increase in glutamate levels, the situation in AD is more complex. This may be due to a difficulty in distinguishing between the primary effects of the tauopathy in AD and secondary homeostatic enhancement as a compensation to loss of function in cortical tangle-bearing neurons. It may lead to compensatory glutamatergic hyperactivity in circuits which remain intact [27,28]. A dysregulation of glutamate release, receptor distribution, transport and uptake are common features of AD [29]. Diminished expression of vesicular glutamate transporter (vGLUT1; [30,31]) or reduced uptake through the excitatory amino acid transporter 2 (EAAT2; [32,33]) could lead to increased glutamate levels in the presynapse, reduced clearance from the synaptic cleft and excessive entry of Ca^{2+} ions through post-synaptic NMDA receptors, and hence provide an explanation for the utility of memantine in AD [34,35]. Cryopreserved synaptosomes from the brains of AD patients show a release of truncated tau fragments from presynaptic terminals [36], suggesting a relationship between transmitter release and tau propagation. Tau has been reported to be in different tau forms in pre- and postsynaptic compartments [36–39].

Some light has been shed on abnormalities in glutamate physiology from studies in tau transgenic mice. Most studies on glutamate release in tauopathy models to date have focused on mutations of tau at position P301 which is present in some bvFTD cases but not in AD. Tau pathology in tau transgenic models in which tau aggregation is expressed in astrocytes (using either the mouse prion promoter [40] or the GFAP promoter [41]) produces impairment in glutamate clearance via reduction in expression of GLUT1, the principal transporter required for astrocytic glutamate uptake. In the tau P301L Tg4510 mouse model, a 40% increase in hippocampal VGLUT1 and a 40% decrease in glutamate transporter 1 (GLT-1) has been demonstrated [40,42,43], suggesting that tau may contribute directly to glutamate excitotoxicity through elevated glutamate vesicle packing and reduced glutamate clearance from the extracellular space. This hyperactivity of glutamatergic release may drive the release of pathological tau from the presynapse [44,62], contributing to the spread of tau through neuronal connections between anatomically connected brain regions. This extracellular tau, or fragments thereof, may provoke acute presynaptic deficits in transmitter release from hippocampal synaptosomes along with loss of mitochondria, deregulation of presynaptic proteins and alterations in calcium homeostasis [45].

We have previously reported the characterisation of two mouse models which demonstrate transgene-dependent differences in their phenotypic expression [46]. In the L1 mouse, there is overexpression of tau296–390, a core component of the paired helical filaments (PHFs) characteristic of AD. These mice show a deficit in spatial learning and memory from 3 months onwards and the spread of pathology from medial temporal lobe structures to isocortex as the animals age that is

somewhat characteristic of the Braak staging of tau pathology observed in AD [47]. L66 mice express full-length human tau carrying two mutations (P301S/G335D). These mice show aggressive early-onset neurofibrillary degeneration, but the behavioural phenotype is largely in the motor function domain. We have further reported that the tau aggregation inhibitor, hydromethylthioninium mesylate (HMTM), reduces tau aggregation pathology and reverses behavioural deficits in both mouse models [48]. We have also reported recently that HMTM produces very similar exposure-dependent benefits on clinical decline and brain atrophy in both AD and bvFTD [49,50].

Given the similarity of the benefits of HMTM in both AD and bvFTD clinically and in the corresponding tau transgenic mouse models, and the importance of glutamate in learning and memory via its role as the primary neurotransmitter of cortical and hippocampal pyramidal neurons [16], we sought to determine how differential overexpression of tau species involved in AD and bvFTD affect basal glutamate release in synaptosomes prepared from two tau transgenic models (L1 and L66) with and without HMTM treatment. Functional assessment of glutamate release from the presynapse can be achieved indirectly through potassium chloride challenge of intact, viable synaptosomes [51,52]. We demonstrate that there is a reduction in synaptic glutamate release in synaptosomes from the brains of the AD-like, L1 mice which is Ca^{2+} -independent and, following HMTM treatment, is normalised to wild-type levels. In contrast, for synaptosomes from the FTD-like L66 mice, glutamate release is increased, remains sensitive to Ca^{2+} and also is normalised by HMTM treatment. The ability of HMTM to reverse opposite abnormalities in glutamate release in both mouse models may provide a possible explanation for the similarity of the HMTM exposure-dependent pharmacological activity observed in both AD and bvFTD.

2. Materials and methods

2.1. Transgenic animals

Female homozygous transgenic L1, L66 and wild-type (NMRI) litters were generated as previously described [46]. L1 mice express truncated tau296–390 fused with an N-terminal endoplasmic reticulum-directing signal sequence while L66 mice express full-length human tau40 (htau40; 1–441 amino acids) carrying two mutations (P301S and G335D). Transgene constructs were inserted under the control of the murine Thy1 cassette, for neuronal expression. All animals were bred commercially at Charles River (UK), and transported to the Medical Research Facility, University of Aberdeen, UK by road about 1 month prior to use to allow for ample acclimatisation. Mice were colony housed (up to 6 per cage) in wire-lid cages (Macrolon III) with corn cob bedding and enrichment (paper strips and cardboard tubes: DBM Scotland Ltd) in a controlled facility (temperature 20–22 °C, 60–65% humidity, 17–20 air changes per hour), with ad libitum access to water and food pellets (Special Diet Services, Witham, UK) and under a 12-h light/dark cycle (lights on at 07:00 am, simulated dawn 30 min). Experiments were carried out in accordance with the European Communities Council Directive (63/2010/EU) and a project license with local ethical approval under the UK Animals (Scientific Procedures) Act (1986) and following Animal Research: Reporting of in vivo Experiments (ARRIVE 2019) guidelines [53].

2.2. HMTM treatment and dosing regimen

Animals were allocated to the two treatment groups, HMTM (15 mg/kg; TauRx Therapeutics Ltd.) or vehicle (deionised water) at 6.5 months of age according to genotype. Previous experiments [46,48] had confirmed the establishment of full pathological and behavioural phenotypes at this age. Treatments were administered orally by gavage ($n = 6–8$ per genotype and treatment group, without blinding (since HMTM is turquoise) and no a priori power calculation was conducted. Animals were allocated to dosing group by Latin Square design. HMTM (15 mg/

kg; expressed as weight of free HMT base) was dissolved in nitrogen-sparged water and administered within 20 min of dissolution, to avoid oxidation of HMTM. This dose was selected on the basis of previous experiments [48]. Once administered, HMT remains primarily in the reduced form [54] and is the active species inhibiting tau aggregation *in vitro* [55]. HMTM was administered daily in the morning (08.00–10.00 h), Monday to Friday, for 3 weeks by oral gavage and this was followed by tissue harvest for synaptosomal preparation.

2.3. Synaptosomal preparation

One hour following the final gavage of either HMTM or saline, mice were sacrificed for isolation of P2 synaptosomes. All animals were killed humanely by cervical dislocation followed by decapitation and whole brain dissection. This was carried out in accordance with Schedule 1 from the UK Animals (Regulated Procedures) Act, 1986. All dissection equipment was kept on ice prior to tissue harvest. Once isolated, the whole brain was placed immediately in ice-cold sucrose/EDTA solution (320 mM sucrose, 1 mM EDTA, 5 mM Tris; pH 7.4). The tissue was then homogenised using a 30 ml borosilicate glass homogeniser (Wheaton, USA), using an automatic homogeniser (IKA Eurostar 20, Germany), for 7 up and down strokes, at 700 rpm. All centrifugation steps that followed were carried out at 4 °C (Beckman Avanti, J-20XP centrifuge). The homogenate was centrifuged at 2800 rpm, for 10 min. The supernatant (S1) was kept on ice, and the pellet (P1) was suspended in ice-cold sucrose/EDTA and centrifuged again for 10 min at 2800 rpm. The second supernatant (S2) was also kept on ice, combined with S1 and then centrifuged for 15 min at 13,000 rpm. The resultant pellet and the P1 pellet were combined in Krebs solution (118.5 mM NaCl, 4.7 mM KCl, 1.18 mM MgSO₄, 10 mM glucose, 1 mM Na₂HPO₄, 20 mM HEPES, pH 7.4), and centrifuged for 10 min at 13,000 rpm to obtain a final pellet used as the synaptosomal P2 fraction. Synaptosomes were used either fresh or frozen as aliquots for immunoblotting.

2.4. Lowry protein assay

Protein was determined by the colorimetric Lowry assay (Bio-Rad DC Protein Assay Kit II). In a clear 96-well plate, 5 µl of bovine serum albumin (BSA) standards (0.15–1.5 mg/ml) were added in triplicate. Five µl of synaptosomes were added to the plate, again in triplicate. Twenty-five µl of alkaline copper tartrate solution (Bio-Rad DC), and 200 µl of Folin's phenol reagent (Bio-Rad DC) were loaded into each well, and the plate was incubated for 15 min at room temperature (RT).

Absorbance was determined at 750 nm using a FLUOstar Omega plate reader (BMG Labtech, Germany). Protein concentration was determined from the standard curve and linear regression of the standard absorbance controls. Synaptosomes were then diluted in Krebs solution to 0.6 mg protein/ml, dispensed into 1 ml aliquots and were collected by centrifugation for 4 min at 4500 rpm (Eppendorf 5424/5424R Microfuge). Pellets were kept on ice until ready to use in the glutamate release assay, to prevent degradation. Synaptosomal pellets were also retained fresh at 4 °C for ultrastructure visualisation or frozen at –20 °C for immunoblotting.

2.5. Electron microscopy

Synaptosome P2 pellets (500 µl), were prepared for electron microscopy by adding 500 µl of cacodylate buffer (0.2 M, pH 7.4) and centrifuged briefly. The pellet was fixed by addition of 1 ml of 5% glutaraldehyde (5% in 0.1 M cacodylate; Sigma-Aldrich) for 30 min on ice. Samples were washed 3 × 5 minutes with 0.1 M cacodylate, fixed for 30 min in OsO₄ (1% in 0.1 M cacodylate; Sigma-Aldrich) and washed 2 × 5 min with 0.1 M cacodylate. Synaptosomal preparations were dehydrated gradually in aqueous solutions of ethanol from 30 to 100% (each for 3 min) and then 100% acetone (three changes, each for 3 min). Specimens were infiltrated with a mixture of 50% epoxy resin and 50%

pure acetone for 2 h at RT, then the mixture was replaced with pure resin which was cured at 60 °C for 48 h. Samples were micro-sectioned with a Diatome diamond knife into 70-nm ultrathin sections (Leica UC7 ultramicrotome), collected using slot copper grids with a carbon-coated Pioloform® film and then counterstained with 3.5% aqueous uranyl acetate followed by Reynolds' lead citrate. Sections were viewed on a JEM1400 transmission electron microscope (JEOL) at 80 kV accelerating voltage and images were acquired with an AMT XR60 CCD camera.

2.6. Immunoblotting

Protein concentration for immunoblotting of synaptosomal preparations was determined using a standard bicinchoninic acid assay (BCA). BSA standards (0–1000 µg/ml) were prepared in NP-40 lysis buffer: 1 ml HEPES (1 M), 1.5 ml NaCl (5 M), 50 ml EDTA (0.1 M in 2 M NaOH), 500 ml Igepal (1%), 47 ml distilled water, 1 protease inhibitor tablet and 1 phospho-STOP (Sigma-Aldrich); pH adjusted to 7.6. Standards (10 µl) were added to the wells of a 96-well plate and soluble homogenates (2.5 µl) included in triplicate. BCA (200 µl; Sigma-Aldrich) and 4% cupric sulphate (1:50; Sigma-Aldrich) were loaded into each well, and the plate incubated (30 min at RT). Absorbance at 562 nm was determined using a FLUOstar Omega plate reader (BMG Labtech, Germany).

Samples for electrophoresis were prepared to a final concentration using NuPAGE® lithium dodecyl sulfate (LDS) sample buffer (Invitrogen®) and 15 mM dithiothreitol (DTT; Sigma-Aldrich). Samples (2 µg/µl) were separated by SDS-PAGE (sodium dodecyl sulfate-polyacrylamide) gel electrophoresis using 17-well pre-cast polyacrylamide NuPAGE® Bis-Tris 4–12% (Life Technologies, USA), in MOPS (3-(N-morpholino)propanesulfonic acid; 50 mM; pH 7.5). Magic Mark protein (1.5 µl) and SeeBlue marker (3 µl; Thermo-Fisher Scientific) were included as molecular weight markers. Proteins were transferred from gels onto nitrocellulose membranes (0.45 µm; Thermo-Fisher Scientific), using wet transfer (5% transfer buffer, 20% methanol), for 1 h, 25 mV. Ponceau S Red (Sigma Aldrich) dye was used for immediate protein transfer detection via protein ladders, followed by 3 × 5 minute washes with Tris-buffered saline containing 0.05% Tween 20 (TBST). Membranes were blocked with 5% milk powder (Marvel) in TBST for 1 h at RT. The membranes were incubated with primary antibody (mAbs 27/499 diluted 1:10, or 7/51 diluted 1:20; Wischik et al., 1996) overnight, then secondary antibody (goat anti-mouse horseradish peroxidase HRP (H + L; AP308P, Merck: 1/2500) was applied. Blots were incubated for 1 min in freshly prepared chemiluminescence substrate reagent (0.015% hydrogen peroxide, 30 µM coumeric acid in 1.25 mM luminol; Sigma-Aldrich), and images captured using a digital camera (PEQLAB, BioTechnologie GmbH, Germany) with auto exposure set for high sensitivity. Exposure times were adjusted according to image saturation. Blots were normalised using Coomassie blue staining as a loading control.

Membranes were stained in Coomassie blue (0.2% solution; x1 Coomassie tablet; PhastGelBlue-R350 (GE Healthcare), 80 ml distilled water, 120 ml methanol) for 1 min to allow visualisation of protein bands, washed (20 ml ethanol, 16 ml water, 4 ml acetic acid) on a rocker for 15–20 min, rinsed with water and allowed to dry. Images were obtained by HP Scanjet. Densitometric analysis of 16-bit immunoblot images was carried out using ImageJ (NIH) software.

For quantification of the L1-specific tau296–390 fragment, synaptosome preparations were prepared at 3 µg/µl in sample buffer (Thermo Scientific non-reducing Sample buffer Cat # 11819340). The protein concentration was determined by BCA analysis and 10 µl/30 µg total protein was loaded per lane. Samples were separated on Bio-Rad Any Kd TGx Criterion gels (Bio-Rad Cat # 5671125) at 70 mA constant current for 30 min and transferred to 0.2 µm PVDF membranes using Bio-Rad Trans Blot Turbo Transfer System and reagents on the mixed Mr. program 2.5 A, 25 V, for 7 min.

Membranes were first labelled with anti-tau antibody S1G2 which was raised against tau297–391 (sheep mouse chimeric IgG2a produced

by Scottish Biologics Facility Aberdeen University, details to be published paper in preparation) using the following protocol. Membranes were blocked for 1 h at room temperature in blocking buffer (5% Marvel dried milk powder in PBS 0.1% Tween20) and then incubated overnight at 4 °C with 1:5000 (0.2 µg/mL) S1G2 diluted in blocking buffer. Membranes were washed 5× with PBST and labelled with goat anti-mouse IgG HRP-conjugated second antibody (Bio-Rad Cat # 1706516) diluted 1:20,000 in blocking buffer for 1 h at room temperature. After washing 5× with PBST, membranes were developed using Clarity ECL substrate (Bio-Rad Cat # 1705061) and imaged with UVP Biospectrum 810 and tau-immunoreactive bands quantified using UVP Visionworks LS v8.2.

To provide a loading control, membranes were then re-probed with rabbit anti-synaptophysin (1:2000; SYSY cat no 101002) followed by goat anti-rabbit IgG HRP-conjugated secondary antibody (1:10,000; Biorad Cat #1721019) using the same protocol as above.

2.7. Glutamate release assay

Potassium (K^+) chloride-dependent glutamate release was quantified indirectly through enzyme-linked spectrofluorimetry. Synaptosomes (0.6 mg in 2 ml) were suspended in Krebs solution, either in the presence of Ca^{2+} (0.4 mM $CaCl_2$) or its absence (including 1 mM EGTA (ethylene glycol-bis (β -aminoethyl ether)- N,N,N',N' -tetraacetic acid, Sigma-Aldrich) at 37 °C, in 3.5 ml flat-bottomed cuvettes (Starna Scientific Ltd). Experiments were started at $t = 0$ by the addition of $NADP^+$ (1 mM; Sigma-Aldrich) to synaptosomes with an 8-mm magnetic stirrer (Fisher Scientific, UK) in the sample chamber of the spectrofluorometer (Photo Technology International Deltascan Model 4000–45). After equilibrium reached, at $t = 60$ min, glutamate dehydrogenase (50 U/ml) was added to the synaptosome suspension, and stimulation initiated at $t = 240$ min by the addition of KCl (30 mM). Fluorescence was recorded at $\lambda_{exc} = 340$ nm, $\lambda_{em} = 460$ nm. Experiments were standardised by the addition of L-glutamate (0.5 mM) at $t = 660$ min and recordings terminated at $t = 900$ min. Data were collected at 1-s intervals.

2.8. Quantification of synaptosomal glutamate release

Traces were saved in ASCII format (Lab Master Series Software, version 1.22, 1986; Scientific Solutions® Inc.) and exported to Microsoft Excel. Raw absorbance was converted to glutamate release (according to 0.6 mg/ml per synaptosome) after alignment of all traces to 240 min, followed by quantification of the time point at which the 0.5 mM glutamate standard is added ($t = 660$ min to $t = 900$ min), and then by normalisation of fluorescence to WT. Quantification of glutamate release (nmol/mg) was calculated for 0.6 mg/ml per synaptosome. Maximal release is presented as values derived from $t = 660$ minus those from $t = 240$ for quantification of K^+ -evoked glutamate release. All traces were smoothed to reduce noise artefacts, using second-order polynomial smoothing (GraphPad Prism 8).

2.9. Statistical analysis

All data are expressed as mean \pm standard deviation (SD) for the number of experiments indicated in both figure and table legends. Data were analysed using 1-way ANOVA, followed by planned post-hoc comparisons using two-tailed Student's t -tests, or repeated measures 2-way or 3-way ANOVA for multiple comparisons, followed by post-hoc comparison using multiple t -tests, as appropriate. The differences between means were considered statistically significant when $*p < 0.05$. Statistical outliers were removed using Grubbs test. All statistical analyses were carried out using GraphPad Prism Software (Version 8; GraphPad Software, San Diego, USA).

3. Results

3.1. Body weight remains stable following repeated HMTM dosing in transgenic L1 and L66 mice

Prior to gavage, both transgenic lines were significantly smaller and presented with reduced body weights compared with wild-type (WT) mice (Fig. 1A). Following the 3-week HMTM (15 mg/kg) dosing period, body weight appeared relatively stable in both vehicle- and HMTM-treated groups (no effects of days) in all genotypes (Fig. 1B–D). In addition, no significant difference between treatments (HMTM 15 mg versus vehicle) was observed, indicating that oral gavage of HMTM was tolerated by both transgenic and WT animals.

3.2. Abundance of synaptosomes obtained in the synaptosomal P2 fraction

The ultrastructure of synaptosomes was investigated for WT mice (6.5 months old) using electron microscopy. The P2 pellet was enriched in synaptosomes, with several intact, sealed synaptosomes (Fig. 2A, framed in black, and B), but it also contained pieces of non-myelinated (pre, Fig. 2A) and myelinated axons (Mem, Fig. 2A), and numerous mitochondria (*, Fig. 2A–B) either free floating or located inside structures. Higher magnification underlined the existence of intact P2-enriched presynaptic glutamatergic synaptosomes containing both post-synaptic densities (black arrows, Fig. 2B) and a large vesicle pool (white arrows, Fig. 2B). Mitochondria (* in Fig. 2B) were also confirmed. These data establish that the P2 fraction contains morphologically complete glutamatergic synaptosomes with intact post-synaptic connections that makes it suitable for the measurement of glutamate release from these structures.

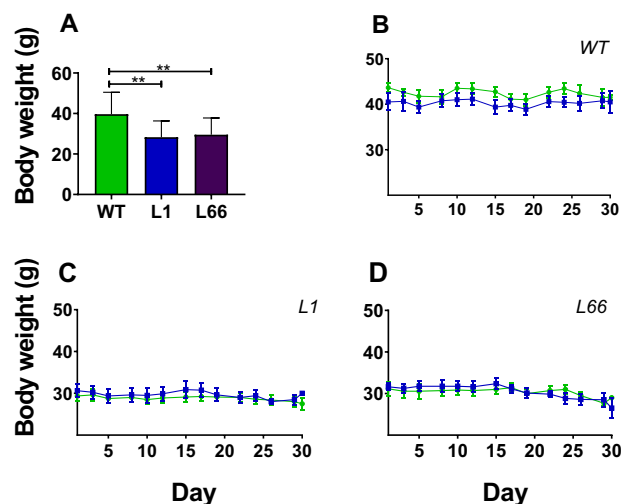


Fig. 1. (A) Body weight of L1, L66 and WT mice prior to treatment at 6.5 months of age. Overall effect of genotype was determined using 1-way ANOVA ($p < 0.01$), followed by post-hoc comparison using t -tests with control as pre-specified comparator (**, $p < 0.01$). Body weight over the 3-week dosing period for (B) WT, (C) L1, and (D) L66 mice at 6.5 months for groups treated with either vehicle (green) or HMTM (15 mg/kg) (blue). Overall effect of treatment was determined using either 1-way ANOVA followed by two-tailed Student's t -test (A) or 2-way ANOVA (B–D): all F values < 1 , p values > 0.05 . All data presented as mean \pm SD with individual scatter (A). (For interpretation of the references to colour in this figure legend, the reader is referred to the web version of this article.)

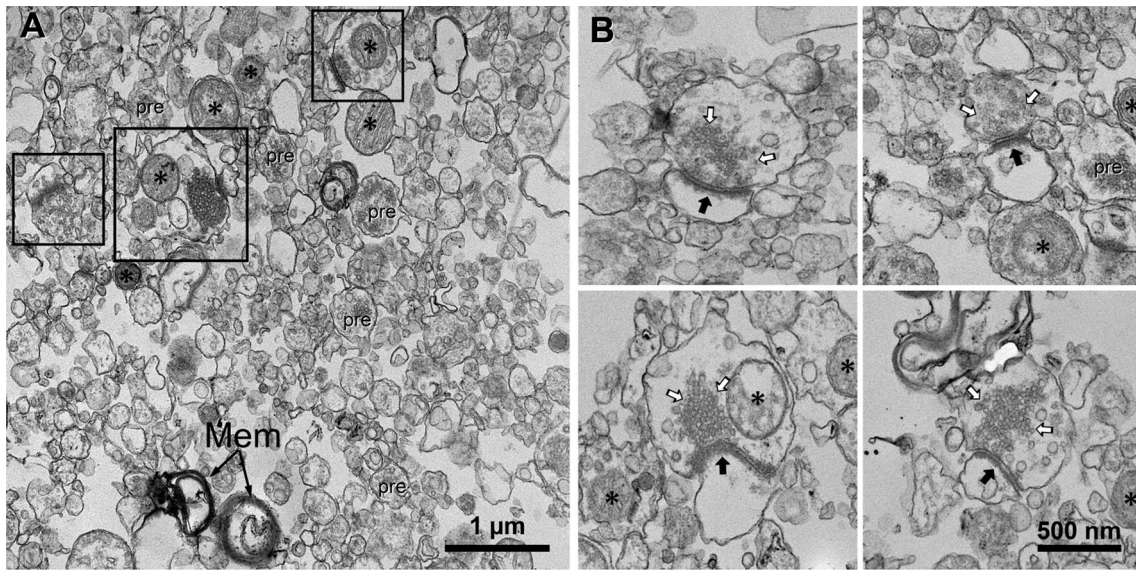


Fig. 2. Electron micrographs of 70-nm ultrathin sections from P2 synaptosomes from WT mice at 6–7 months.

(A) Electron micrograph displaying intact synaptosomes (framed in black) alongside identifiable presynaptic boutons (pre), mitochondria (*), and large structures encircled with membrane such as myelin (Mem). (B) Magnified electron micrographs of individual, intact P2 synaptosomes and synaptic vesicles. Pre-synaptic vesicles are indicated by white arrows, while the post-synaptic densities are marked by black arrows. Mitochondria are labelled by asterisks (*).

3.3. Tau levels in synaptosomal preparations were reduced following HMTM treatment

We next determined whether synaptosomes derived from transgenic mice were enriched for tau, and whether this can be lowered by long-term treatment with HMTM. Tau levels were investigated in P2 synaptosomes isolated from WT, L1 and L66 mice, at 6 months of age. In L66

mice, human tau having a gel mobility of 65–70 kDa was detected in synaptosomes using mAb 27/499, an antibody that recognises a human-specific epitope near the N-terminus (Wischnik et al. 1996). This was absent in synaptosomes from WT and L1 mice (Fig. 3A; hTau40). The mAb 7/51, which recognises a generic tau epitope within the repeat domain (residues 315–376) (Harrington et al. 1991), detected endogenous mouse tau with mobility of 50 kDa in all genotypes (WT, L1 and

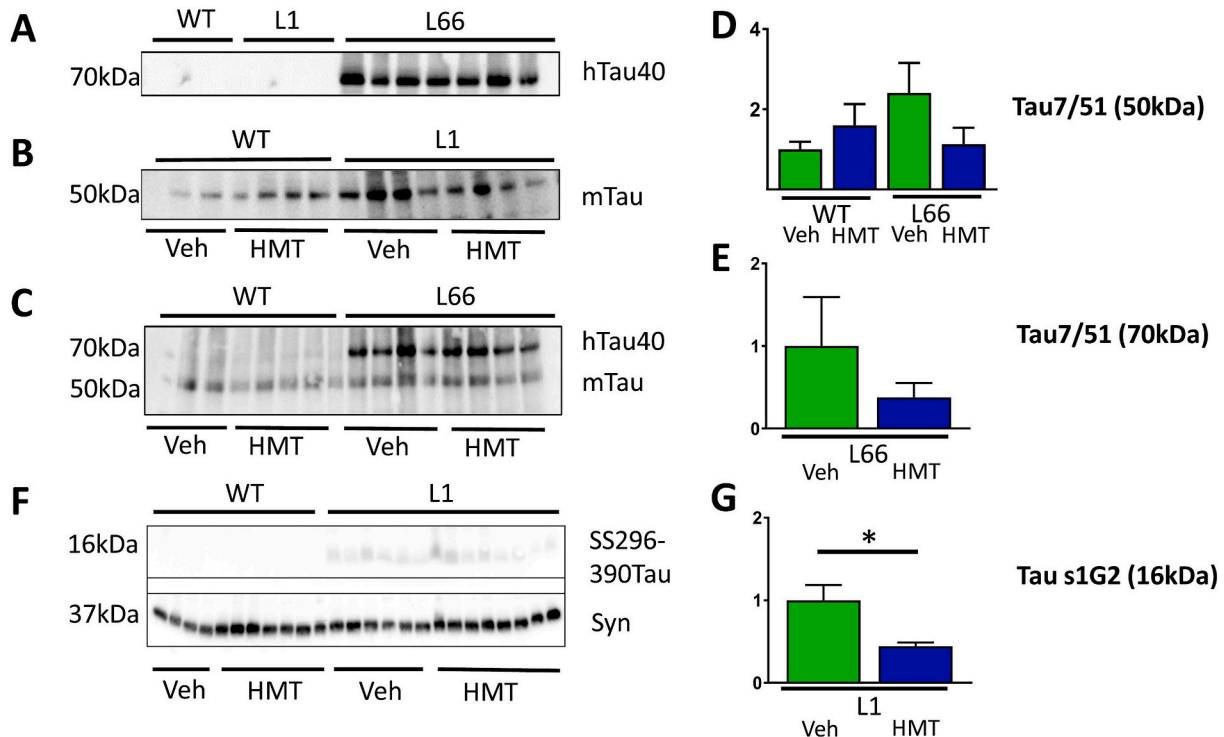


Fig. 3. Tau immunoblots of synaptosomes using mAbs 499 (A) and 7/51 (B, C) and quantification of tau (D, E) in P2 synaptosomal pellets in WT ($n = 4$), L1 ($n = 4$) and L66 ($n = 4$) animals, each aged 6 months. Bands at 50 kDa (B, C, D) and 70 kDa (A, C, E) indicate endogenous murine and transgenic human tau, respectively. (F) S1G2 labelled truncated tau296–390 in synaptosomes from L1 but not WT. (G) There was a significant decrease in human tau in the presence of HMTM ($n = 5$, veh; and $n = 7$, HMTM). Data were normalised to total protein load (Coomassie stain control, not shown), except for (F), where data were normalised to synaptophysin (Syn). Differences were considered statistically significant when $*p < 0.05$ using two-tailed Student’s t-test. Data are presented as mean values + SD.

L66; Fig. 3B). Increased levels were detected in the 50-kDa mouse tau band in L1 synaptosomes compared with those from WT mice (Fig. 3B). No significant differences were detected in the HMTM (15 mg/kg)-treated groups compared to vehicle controls for either L1 or WT mice (Fig. 3B). For L66 synaptosomes, mAb 7/51 detected full-length human tau (ca. 65–70 kDa) that was not observed in WT synaptosomes from animals of the same age (Fig. 3C; hTau40). The mAb 7/51 also detected 50-kDa tau in both L66 and WT synaptosomes (Fig. 3C). No statistical differences, however, were observed across genotype or treatment group for the 7/51-reactive 50-kDa band (Fig. 3D). There was a directional reduction in the 65–70 kDa band in HMTM-treated mice, although this did not reach statistical significance (Fig. 3E). The truncated tau in L1 was visualised with the mAb S1G2 (raised against tau297–391) (Fig. 3F) but absent in WT controls. HMTM significantly reduced levels of the tau296–390 fragment in L1 (Fig. 3G; $p = 0.019$). Data suggest that HMTM did reduce the levels of the transgenic tau species in both L66 and L1.

3.4. Basal glutamate release in synaptosomes from AD and FTD mouse models mirrors the distinctive glutamate abnormalities of each disease

This study was conducted as a single experiment. A counterbalanced Latin square design was implemented with all genotypes and treatments included. Consequently, all data were acquired at the same time to avoid variability due to repetitions. However, for clarity, the data have been broken down into fragments below to accommodate the research questions asked.

In order to determine whether basal glutamate release differed in transgenic L1 and L66 mice compared with WT mice, K^+ -evoked glutamate release was measured in synaptosomes prepared from mouse brain tissue harvested from animals at 6–7 months of age. Qualitative analysis of sample traces revealed a strong reduction in K^+ -evoked release of glutamate in synaptosomes from L1 AD mice compared to age-matched WT mice (Fig. 4A; compare blue and green lines, respectively). By contrast, K^+ -evoked glutamate release in L66 FTD mice was enhanced (Fig. 4A purple line). A main effect of genotype (1-way ANOVA; $F_{(2,19)} = 3.019$; $p < 0.01$) was significant and pairwise comparisons confirmed that both the reduction in the AD-like mice and the increase in the FTD-like mice were significant compared with WT control mice (see asterisks in Fig. 4B). Therefore, overexpression of different pathogenic tau species in the two models produces distinct abnormalities in glutamate release from synaptosomes.

One potential mechanism responsible for these divergent tau transgene effects may be their Ca^{2+} dependence. Typically, K^+ -evoked release of glutamate is dependent on the influx of extracellular Ca^{2+}

which triggers a continuous rise in transmitter release. This response can be blocked by adding the Ca^{2+} -chelator EGTA to the medium. As expected, Ca^{2+} -dependent glutamate release was reduced by EGTA in WT mice (Fig. 5A – red line). The same strong reduction in glutamate release was also seen in synaptosomes from L66 mice (Fig. 5C – red line). Surprisingly, adding EGTA had no effect on glutamate release in L1 mice (Fig. 5B – red line). These differences were confirmed statistically using a factorial 2-way ANOVA (Fig. 5D; treatment, $F_{(2,38)} = 7.314$; $p < 0.01$; genotype, $F_{(2,38)} = 5.755$; $p < 0.01$). Post-hoc analyses confirmed that the pairwise EGTA-dependent differences were each significant in WT and L66 mice, but not in L1 mice (Fig. 5D – asterisks). Therefore, the abnormally increased glutamate release seen in the FTD mouse model retains normal dependence on extracellular Ca^{2+} . By contrast, the reduction K^+ -evoked glutamate release seen in the AD mouse model is not sensitive to reduction in extracellular Ca^{2+} , implying a defect either in the voltage-gated Ca^{2+} channel or an impairment in glutamate release mechanisms.

3.5. Chronic pre-treatment with HMTM normalises glutamate release abnormalities in both L1 and L66 mice

Since HMTM has been shown to inhibit pathological aggregation of tau in vitro [55,56] and reduce tau aggregation pathology in both L1 and L66 mouse models following long-term (> 3 weeks) administration of HMTM [48; see Fig. 3], we investigated the effect of chronic pre-treatment with HMTM on the transgene-specific abnormalities in K^+ -evoked glutamate release. The findings are summarised in Fig. 6 for the effect of HMTM treatment on basal K^+ -evoked glutamate release and in Fig. 7 for the effect of EGTA on glutamate release.

A 2-way ANOVA yielded significant effects of both treatment and genotype (treatment, $F_{(6,75)} = 5.077$; $p < 0.001$; genotype, $F_{(2,75)} = 5.840$; $p < 0.01$, respectively). As can be seen from Figs. 6A & D, HMTM marginally reduced glutamate release in synaptosomes from WT mice. In L1 animals however, HMTM treatment led to a significant increase in glutamate release (Figs. 6B & D), bringing the mean level back to that

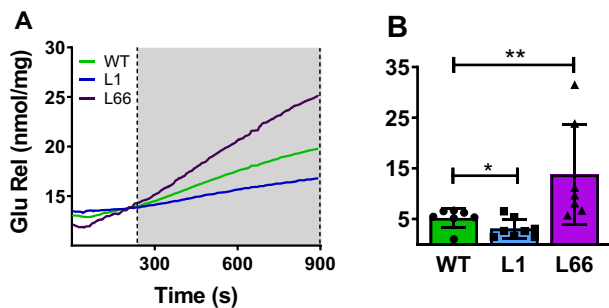


Fig. 4. (A) Ca^{2+} -dependent P2 synaptosomal glutamate release (nmol/mg) in the presence of 0.4 mM $CaCl_2$ in L1 ($n = 8$), L66 ($n = 6$) and WT (NMR; $n = 7$) mice at 6.5 months. Traces represent KCl-evoked glutamate release (T900–T240). Grey box indicates the period over which glutamate release (nmol/mg) was analysed. (B) Glutamate release in L1, L66 and WT animals. Reliability was determined using 1-way ANOVA ($p < 0.01$), and effect of genotype was determined using two-tailed Student's *t*-test. Data presented as mean \pm SD with individual scatter. * $p < 0.05$ and ** $p < 0.01$.

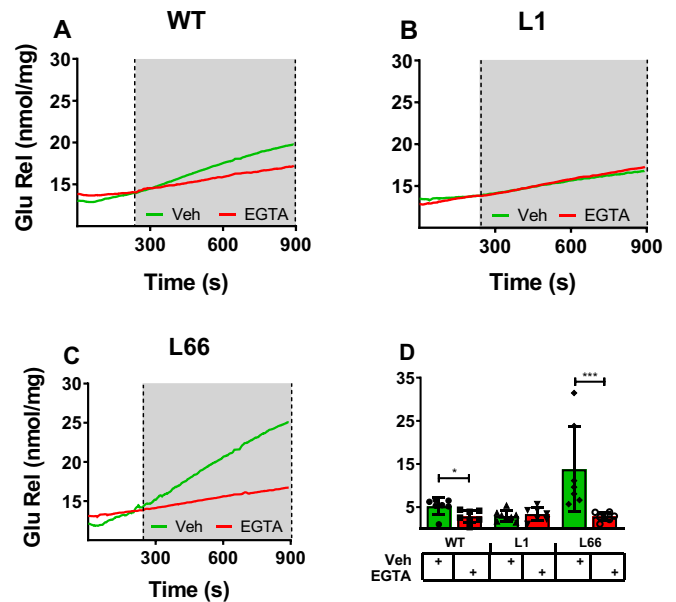


Fig. 5. Ca^{2+} -dependent and independent P2 synaptosomal glutamate release (nmol/mg) in the presence of either 0.4 mM $CaCl_2$ or 1 mM EGTA in (A) WT ($n = 7$) (B) L1 ($n = 8$) and (C) L66 ($n = 6$) mice at 6.5 months. Grey box indicates the period over which glutamate release (nmol/mg) was analysed. (D) Glutamate release in L1, L66 and WT animals. An overall interaction between genotype and treatment was revealed using 2-way ANOVA ($p < 0.01$), and effect of treatment (*). All data presented as mean \pm SD with individual scatter. * $p < 0.05$, ** $p < 0.01$ and *** $p < 0.001$.

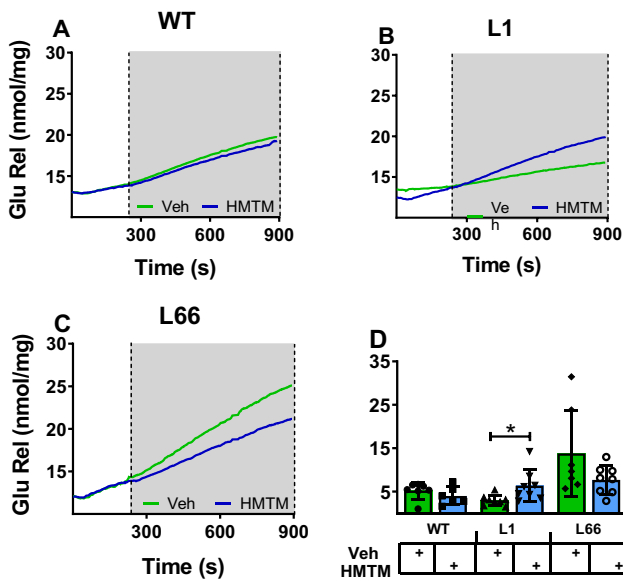


Fig. 6. Ca^{2+} -dependent P2 synaptosomal glutamate release (nmol/mg) in the presence of 0.4 mM CaCl_2 in vehicle- and chronic HMTM (15 mg/kg)-treated (A) WT (NMRI; $n = 7$) (B) L1 ($n = 8$) and (C) L66 ($n = 6$) mice at 6.5 months. Grey box indicates the period over which glutamate release (nmol/mg) was analysed. (D) Glutamate release in L1, L66 and WT animals. An overall interaction between genotype and treatment was confirmed using 2-way ANOVA ($p < 0.001$), and effect of treatment (*) determined using post-hoc multiple t-tests. All data presented as mean \pm SD with individual scatter. * $p < 0.05$, ** $p < 0.01$ and *** $p < 0.001$.

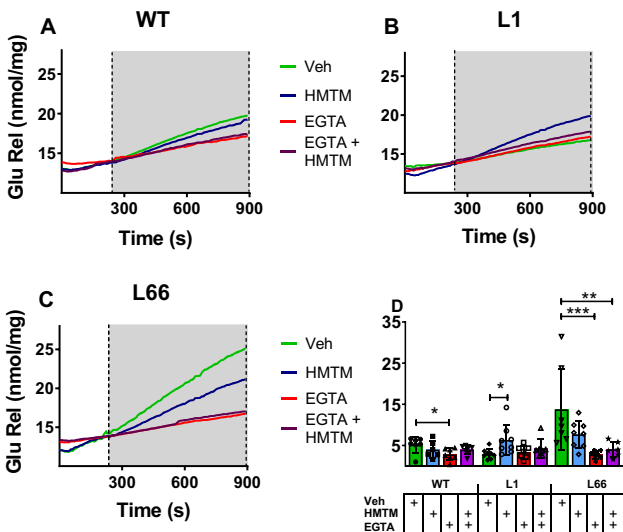


Fig. 7. Ca^{2+} -dependent and independent P2 synaptosomal glutamate release (nmol/mg) in the presence of either 0.4 mM CaCl_2 or 1 mM EGTA in vehicle- or chronic HMTM (15 mg/kg)-treated synaptosomes in (A) WT ($n = 7$) (B) L1 ($n = 8$) and (C) L66 ($n = 6$) mice at 6.5 months. Grey box indicates the period over which glutamate release (nmol/mg) was analysed. (D) Quantification of glutamate release in L1, L66 and WT animals. (+) indicates presence of vehicle, HMTM or EGTA. An overall interaction between genotype and treatment was confirmed using 2-way ANOVA ($p < 0.01$), and effect of treatment determined by post-hoc multiple t-tests. All data presented as mean \pm SD with individual scatter. * $p < 0.05$, ** $p < 0.01$ and *** $p < 0.001$.

seen in WT controls. Post-hoc pairwise comparisons confirmed the significant increase in K^+ -evoked glutamate release in L1 mice following HMTM treatment whereas there was no significant HMTM effect in WT

mice. By contrast, HMTM treatment normalised K^+ -evoked glutamate release in L66 mice bringing it to a level that could no longer be distinguished from WT control mice, although the difference with respect to vehicle-treated L66 controls did not reach statistical significance. Therefore, HMTM treatment normalises K^+ -evoked glutamate release by producing directionally opposite effects in synaptosomes isolated from the AD and FTD mouse models respectively. Furthermore, the results confirm that the abnormalities in glutamate release in both mouse models are dependent on the aggregation of pathogenic tau species.

We further examined how normalisation of glutamate release is linked to Ca^{2+} -dependency. For all groups, a 2-way ANOVA showed that genotype ($F_{(2,75)} = 5.840$; $p < 0.01$) and treatment ($F_{(6,75)} = 5.066$; $p < 0.001$) were both significant. The expected EGTA-induced reduction in glutamate release in WT mice was seen in both vehicle- and HMTM-treated mice, although this achieved significance in the post-hoc pairwise comparisons only in the vehicle-treated mice (Figs. 7A & D). In L1 mice, the significant increase in glutamate release produced by HMTM treatment was eliminated in synaptosomes incubated with EGTA (Figs. 7B & D). This implies that, in the AD mouse model, HMTM treatment both restores K^+ -evoked glutamate release to normal levels and also restores normal Ca^{2+} -dependency in synaptosomes. In synaptosomes from L66 mice, the reduction in K^+ -evoked glutamate release produced by HMTM treatment was further enhanced by addition of EGTA to synaptosome preparations such that the combined effect reached statistical significance in post-hoc pairwise comparisons. This indicates that the normalisation of glutamate release in L66 synaptosomes produced by HMTM pre-treatment was not the result of an interference with normal Ca^{2+} -dependent mechanisms. The directionally opposite glutamate release abnormalities produced in the two tau transgenic mouse models were each reversed by HMTM.

4. Discussion

We have previously reported two different tau transgenic mouse models (L1 and L66) that display some phenotypic features of AD and FTD, respectively. The findings we now report demonstrate that synaptosomes from brains of these mice present directionally opposite abnormalities in K^+ -evoked glutamate release. The AD L1 mouse model expresses only the core aggregation domain of tau and produces a cognitive defect from as early as 3 months [46]. In synaptosomes isolated from these mice, glutamate release was significantly reduced, and residual K^+ -evoked glutamate release appeared independent of extracellular Ca^{2+} influx. We further report that chronic pre-treatment with the tau aggregation inhibitor HMTM reversed the glutamate release deficit and restored sensitivity to extracellular Ca^{2+} . Therefore, both reduced glutamate release and resistance to chelation of extracellular Ca^{2+} are caused by pathological aggregation of the AD PHF core in this model. Conversely, synaptosomes from the FTD L66 mouse model, expressing a mutant form of full-length tau carrying dual pathogenic mutations at P301S/G335D [46,48], demonstrated excessive K^+ -evoked glutamate release but retained normal Ca^{2+} sensitivity. As with the AD model, chronic pre-treatment with HMTM normalised excessive glutamate release. The results therefore establish that opposite abnormalities in glutamate release seen in the two mouse models are both determined by aggregation of the specific form of pathogenic tau that is expressed in each mouse and that both respond to treatment with HMTM. These results raise the intriguing question as to the mechanisms whereby different forms of oligomeric tau produce such different glutamate release abnormalities but which both remain responsive to treatment with HMTM. We have previously shown that HMTM is a potent tau aggregation inhibitor in vitro and in vivo [48,55,56] and that it reduces clinical decline and brain atrophy in a similar concentration-dependent manner in both AD and bvFTD [49,50]. The fact that normalisation of glutamate release can be achieved by blocking tau aggregation implies that pathological aggregation of tau can affect synaptic function in

different ways that are specific to the tau species that accumulate in each disease.

The two main differences in the transgenes we have used are that, in the bvFTD model, the tau is full-length carrying two mutations in the repeat domain whereas, in the AD model, the tau is truncated but without any mutations. The filaments in the brains of subjects with AD and bvFTD differ in structure. In AD, the filaments are predominantly PHFs, whereas those in Pick disease are straight filaments [57,58]. Furthermore, the core tau unit expressed in L1 mice has been shown to form PHFs in vitro [59]. Multiple conformations of tau, however, may exist in high molecular weight soluble tau oligomers [60].

The more likely factor responsible for differences in effects on glutamate release is the presence or absence of domains outside the core repeat domain which may be subject to further secondary post-translational modifications including phosphorylation [39]. We have shown previously that the core tau unit is present in synaptic boutons in L1 mice, and that the normal quantitative relationship among synaptic proteins is severely disturbed in the ventral striatum of L1 mice [61]. Likewise, we and others have shown that mutant full-length tau accumulates in synaptosomes from the L66-like mouse models with mutation of Pro-301 [62] and is abnormally phosphorylated [39,62]. Therefore, although different species of oligomeric tau are found within synapses and synaptosomes in these mouse models, they are able to exert different effects on both the Ca^{2+} -dependence and magnitude of the glutamate response to a K^{+} pulse.

We consider Ca^{2+} -dependency first. As far as we are aware, no work has been published on Ca^{2+} responses in any tauopathy models. Compromised calcium signalling is among the earliest events underlying synaptic pathology in AD [64,65]. A possible role for voltage-dependent calcium channels, presumably Cav2.1 and Cav2.2 (P/Q-type and N-type), at glutamatergic synapses has been suggested (see [66] for recent review). The role of these channels is to transduce the incoming electrical signal into ionic influx and thereby promote the vesicular fusion to the presynaptic membrane, triggering neurotransmitter release. The transduction of the K^{+} -pulse into a neurotransmitter response is non-linear and very few Cav 2.2 and Cav 2.3 channels, which cluster randomly around vesicles, can induce release from multiple glutamate-containing vesicles [67]. In addition to the location of the Cav around the active presynaptic zone, the number and density of Cav channels and the coupling distance (distance between Cav channels and exocytotic release sites) are critical for fast release and may be compromised by the exact presynaptic localisation of tau oligomers in L1 mice. The role of Ca^{2+} in different brain regions may differ [68]. While a persistent increase in presynaptic Cav 2.2-mediated transients was recorded at mossy fibre dentate gyrus synapses [69], no change in Ca^{2+} transients were noted during synaptic potentiation applied at cerebellar parallel fibre to Purkinje cells [70].

In synaptosomes from L66 mice, EGTA reduces the K^{+} -evoked glutamate response and brings it to the same level as in WT control mice. Therefore, there does not appear to be any inherent impairment in the functioning of the voltage-dependent calcium channels in L66 mice. The same is true following HMTM treatment, implying that HMTM also does not affect the functioning of the channel. By contrast, chelation of extrasynaptosomal Ca^{2+} has no effect in L1 mice. This lack of response could be due either to dysfunction of these channels caused by truncated tau oligomers, or to dysfunction in downstream Ca^{2+} -dependent effector mechanisms needed for glutamate release. Since the data indicate that normal Ca^{2+} -dependence is restored following HMTM treatment, we can conclude that oligomerisation of truncated tau in L1 mice is responsible for the dysfunction but does not explain the mechanism. However, we have shown previously that there is a substantial disturbance in the quantitative relationships among proteins of the SNARE (soluble N-ethylmaleimide-sensitive factor attachment protein receptor protein) complex in the ventral striatum of L1 mice and presumably elsewhere [61]. This would support the idea that oligomers of truncated tau, but not full-length tau, interfere with the synaptic machinery needed for

vesicles to fuse with the synaptic membrane and release glutamate. We cannot make any predictions as to how this alteration in glutamate release in L1 of L66 correlates with putative tau release and its propagation, but the synaptic localisation of high levels of human tau in both mouse lines corroborates previous work by Mazzo et al. [63] and Kremer and co-workers [62]. Although we have demonstrated intact synaptic vesicles in presynaptic compartments, we did not simultaneously label the sub-compartmental expression and putative species of tau. However, synaptic expression of tau in both our transgenic mouse lines has been proven previously [71].

We next consider the direction of the K^{+} -evoked glutamate response. To date, studies on glutamate release in tauopathy models have focussed predominantly on mutations of tau at the Pro-301 position, including L66 mice. Heightened glutamate signalling has been widely confirmed in these models, although available data relate mostly to postsynaptic signalling cascades mediated through NMDA receptors [72]. However, there are also contradictory findings. Strongly reduced releasable pools of glutamatergic vesicles were observed in aged rTg4510 mice (expressing P301L, [73]), resulting in an overall reduction of glutamate release from the presynapse. When studying the hippocampus in the same mouse model, Hunsberger [40] confirmed a 4- and 7-fold increase in K^{+} -evoked glutamate release in the dentate gyrus and CA3, respectively, as an early event during the progression of tau pathology. Shimjo [74] suggested this hyperexcitability was due to a reduction of inhibitory synapses during ageing. In the hT-337 M mouse model, Warmus and colleagues [75] reported diminished expression of both GluR1, GluR2 and GluN1, GluN2A, GluN2B in synaptosomes from the ventral striatum and insular cortex at 14 months of age, together with lowered input-output relationships in neurons and impaired network activity of the ventral striatum. Hill and colleagues [76] loaded mouse CA1 hippocampus pyramidal or cortical layer V tufted pyramidal cells with oligomeric full-length 2N4R tau through patch clamp pipettes while at the same time recording their action potential. They reported reduced action potential amplitudes and greater run-down of presynaptic unitary excitatory post-synaptic potentials relative to control neurons in both regions tested. Moreover, no effect on basal synaptic transmission was observed by introduction of oligomeric 2N4R tau into the post-synapse but impaired high frequency induced synaptic potentiation [76,77], an observation consistent with a number of studies with mice expressing N-terminal or C-terminal tau fragments in neuronal tissue [45,76,78,79].

The increase in the K^{+} -evoked glutamate response seen in the L66 mice is therefore consistent with some, but not all, of the studies reported to date. The fact that HMTM reduces both the magnitude of the evoked response and the levels of both mutant tau and endogenous mouse tau found in synaptosomal extracts point to a cytoskeletal mechanism. Increased tau in synaptosomal preparations is consistent with recent work by Zhou and co-workers [38] who found in mutant tau models (0N4R tau carrying R406W, V337M and P301L mutations) of both *Drosophila* and mouse that pathological tau mislocalises to presynaptic terminals where it promotes presynaptic actin polymerisation to crosslink vesicles and restrict mobilisation. Disruption of this interaction is sufficient to rescue the defect, a result similar to that seen with HMTM. In addition, mutant human iPSC cells expressing the V337M mutation show impaired activity-dependent plasticity of the cytoskeleton particularly in the axonal initial segment. This impairment resulted in neural hyperactivity in response to continuous depolarisation in line with increased accumulation of structural components of the axonal initial segment such as end-binding proteins [80]. In the hippocampus of P301L (pR5) mice, where expression levels of mutant tau are greatest, overall glutamate homeostasis was found to be disrupted with significant reduction in glutamate levels [81]. However, this is in contrast with the cortex in these pR5 mice, in which radiolabelled glutamate, glutamine and GABA were increased in both neurons and astrocytes. This suggests there is heightened glutamate turnover due to hyperexcitation in the cortex of these mice. However, diminished glutamate release and

impairment in hippocampal synaptic plasticity have also been reported in full-length human tau mouse models [77]. Overall, a plausible hypothesis might be that mislocalisation of full-length mutant tau disturbs the normal control and transport of glutamate vesicle populations resulting in increased numbers in synapses and in synaptosomal extracts. The normalisation of this following HMTM would then be consistent with the reduction in levels of mutant tau pathology in L66 mice.

Although the tissues we have studied were not micro-dissected to differentiate cortical from other brain regions, it is likely that, similar to the rat [82], the neocortex contributes to >30% of the total brain mass of the mice, and therefore constitutes the largest contribution to glutamatergic synapses, i.e. to the results that we report. Ultra-thin sections of our synaptosome preparation revealed dense vesicular pools in the presynapse of EM micro-photographs and confirmed the widespread presence of asymmetrical synapses with post-synaptic densities typical of excitatory synapses and in line with previous reports [83]. Other potential weaknesses in the present study relate to the incomplete characterisation of transgenic tau species in the synaptosomal preparations, particularly those from L1 mice. There were only low levels of the tau296–390 fragment in line 1 but these levels were lowered with HMTM; other tau species await more detailed analysis. A more complete characterisation of tau protein in L66 mice has been reported recently [39] showing that the human tau is insoluble and abnormally phosphorylated in similar synaptosomal preparations. Although the significant elevation in glutamate release from L66 synaptosomes compared with those from wild-type control mice was eliminated by HMTM treatment, the reduction compared to vehicle-treated L66 control did not reach statistical significance and would require confirmation in a larger study.

In summary, we present several new and surprising results showing that different forms of pathogenic tau induce completely different patterns of abnormality in glutamate release in synaptosomes isolated from brains of tau transgenic mice. In the L1 AD mouse model, truncated tau is responsible for impairment in K^+ -evoked glutamate response and loss of Ca^{2+} -dependency. Both these abnormalities can be corrected by chronic pre-treatment with HMTM, implying that oligomers of truncated tau are responsible. We hypothesise, in light of the disturbance in the quantitative relationships among members of the SNARE complex in the L1 mouse that we have recently reported [71], that the primary site of the disturbance is in the mechanisms responsible for the transport and membrane fusion of vesicles that are needed to permit K^+ -evoked glutamate release to occur. In the L66 FTD model, on the other hand, the primary abnormality is one of glutamate hypersecretion, consistent with imaging and post-mortem studies in bvFTD. This abnormality is also driven by pathological aggregation of tau since it can be reversed by prior chronic treatment with HMTM. We hypothesise that the difference in the effects of aggregated tau is determined largely by whether the aggregating species is full-length or truncated, although a subtle effect of the mutations or different folding conformations within the core aggregation domain cannot be ruled out. Overall, our results lead to the conclusion that the group of diseases known as tauopathies cannot be considered to be a single entity in terms of the downstream effects of pathological aggregation of tau protein. Despite this, directionally opposite disease-associated abnormalities in glutamate release resulting from different forms of pathogenic tau can both be corrected by HMTM. This goes some way towards providing an explanation for the similarity in exposure-dependent activity of HMTM on clinical decline and brain atrophy that we have recently reported in both AD and bvFTD [49,50].

Author contributions

Anna Cranston: conceptualization, methodology, formal analysis, investigation, writing original draft; Igor Kraev, Mike G Stewart, David Horsley, Renato Santos, Soumya Palliyil: methodology, analysis, investigation; Lianne Robinson, Paul Armstrong, Eline Dreesen: investigation;

Charles Harrington: funding acquisition, project administration, writing – review and editing; Claude Wischik: funding acquisition, project administration; Gernot Riedel: funding acquisition, conceptualization, project administration, supervision, writing – review and editing. All authors reviewed and agreed to the published version of the manuscript.

CRediT authorship contribution statement

Anna L. Cranston: Writing – original draft, Methodology, Investigation, Formal analysis, Data curation, Conceptualization. **Igor Kraev:** Methodology, Investigation, Formal analysis, Data curation. **Mike G. Stewart:** Methodology, Investigation, Formal analysis. **David Horsley:** Methodology, Investigation, Formal analysis. **Renato X. Santos:** Methodology, Investigation, Formal analysis. **Lianne Robinson:** Investigation. **Eline Dreesen:** Investigation. **Paul Armstrong:** Investigation. **Soumya Palliyil:** Investigation, Methodology, Writing – review & editing. **Charles R. Harrington:** Writing – review & editing, Project administration, Funding acquisition. **Claude M. Wischik:** Project administration, Funding acquisition. **Gernot Riedel:** Writing – review & editing, Writing – original draft, Supervision, Project administration, Funding acquisition, Conceptualization.

Declaration of Competing Interest

The sponsor was involved in the design of the study; in the collection, analysis, and interpretation of the data; and in the writing of the report. The corresponding author had full access to all the data and had final responsibility for the submission of the report for publication. C.R.H. and C.M.W. are officers in TauRx Therapeutics Ltd., an affiliate of WisTa Laboratories Ltd. G.R. has received funding from TauRx Therapeutics Ltd. D.H., C.R.H., C.M.W., and G.R. are named inventors on patents and patent applications owned by WisTa Laboratories Ltd.

Data availability

Data will be made available on reasonable request.

Acknowledgements

This study was sponsored by WisTa Laboratories Ltd., Singapore (grant PAR1577).

Appendix A. Supplementary data

Supplementary data to this article can be found online at <https://doi.org/10.1016/j.cellsig.2024.111269>.

References

- [1] C.M. Wischik, M. Novak, P.C. Edwards, A. Klug, W. Tichelaar, R.A. Crowther, Structural characterization of the core of the paired helical filament of Alzheimer disease, *Proc. Natl. Acad. Sci.* 85 (1988) 4884–4888, <https://doi.org/10.1073/pnas.85.13.4884>.
- [2] D.C. Perry, J.A. Brown, K.L. Possin, S. Datta, A. Trujillo, A. Radke, A. Karydas, J. Kornak, A.C. Sias, G.D. Rabinovici, M.L. Gorno-Tempini, A.L. Boxer, M. De May, K.P. Rankin, V.E. Sturm, S.E. Lee, B.R. Matthews, A.W. Kao, K.A. Vossel, M. C. Tartaglia, Z.A. Miller, S.W. Seo, M. Sidhu, S.E. Gaus, A.L. Nana, J.N.S. Vargas, J.-H.L. Hwang, R. Ossenkoppele, A.B. Brown, E.J. Huang, G. Coppola, H.J. Rosen, D. Geschwind, J.Q. Trojanowski, L.T. Grinberg, J.H. Kramer, B.L. Miller, W. W. Seeley, Clinicopathological correlations in behavioural variant frontotemporal dementia, *Brain* 140 (2017) 3329–3345, <https://doi.org/10.1093/brain/awx254>.
- [3] C. Ballatore, V.M.Y. Lee, J.Q. Trojanowski, Tau-mediated neurodegeneration in Alzheimer's disease and related disorders, *Nat. Rev. Neurosci.* 8 (2007) 663–672, <https://doi.org/10.1038/nrn2194>.
- [4] S. Ghosh, C.F. Lippa, Clinical subtypes of frontotemporal dementia, *Am. J. Alzheimer's Dis. Other Dementias.* 30 (2015) 653–661, <https://doi.org/10.1177/1533317513494442>.
- [5] D. Lewis, M. Campbell, R. Terry, J. Morrison, Laminar and regional distributions of neurofibrillary tangles and neuritic plaques in Alzheimer's disease: a quantitative study of visual and auditory cortices, *J. Neurosci.* 7 (1987) 1799–1808, <https://doi.org/10.1523/JNEUROSCI.07-06-01799.1987>.

- [6] M. Padurariu, A. Giobica, I. Mavroudis, D. Fotiou, S. Baloyannis, Hippocampal neuronal loss in the CA1 and CA3 areas of Alzheimer's disease patients, *Psychiatr. Danub.* 24 (2012) 152–158, <http://www.ncbi.nlm.nih.gov/pubmed/22706413>.
- [7] P.R. Hof, C. Bouras, D.P. Perl, J.H. Morrison, Quantitative neuropathologic analysis of Pick's disease cases: cortical distribution of pick bodies and coexistence with Alzheimer's disease, *Acta Neuropathol.* 87 (1994) 115–124, <https://doi.org/10.1007/BF00296179>.
- [8] G.M. Halliday, Y.J.C. Song, G. Lepar, W.S. Brooks, J.B. Kwok, C. Kersaitis, G. Gregory, C.E. Shepherd, F. Rahimi, P.R. Schofield, J.J. Kril, Pick bodies in a family with presenilin-1 Alzheimer's disease, *Ann. Neurol.* 57 (2005) 139–143, <https://doi.org/10.1002/ana.20366>.
- [9] I. Ferrer, A. Legati, J.C. García-Monco, M. Gomez-Beldarrain, M. Carmona, R. Blanco, W.W. Seeley, G. Coppola, Familial behavioral variant frontotemporal dementia associated with astrocyte-predominant tauopathy, *J. Neuropathol. Exp. Neurol.* 74 (2015) 370–379, <https://doi.org/10.1097/NEN.000000000000180>.
- [10] M. Broe, Astrocytic degeneration relates to the severity of disease in frontotemporal dementia, *Brain* 127 (2004) 2214–2220, <https://doi.org/10.1093/brain/awh250>.
- [11] E.D. Huey, K.T. Putnam, J. Grafman, A systematic review of neurotransmitter deficits and treatments in frontotemporal dementia, *Neurology* 66 (2006) 17–22, <https://doi.org/10.1212/01.wnl.0000191304.55196.4d>.
- [12] P. Davies, A. Maloney, Selective loss of central cholinergic neurons in Alzheimer's disease, *Lancet* 308 (1976) 1403, [https://doi.org/10.1016/S0140-6736\(76\)91936-X](https://doi.org/10.1016/S0140-6736(76)91936-X).
- [13] J.T. O'Brien, A. Burns, Clinical practice with anti-dementia drugs: a revised (second) consensus statement from the British Association for Psychopharmacology, *J. Psychopharmacol.* 25 (2011) 997–1019, <https://doi.org/10.1177/0269881110387547>.
- [14] A.L. Boxer, D.S. Knopman, D.I. Kaufer, M. Grossman, C. Onyike, N. Graf-Radford, M. Mendez, D. Kerwin, A. Lerner, C.K. Wu, M. Koestler, J. Shapira, K. Sullivan, K. Klepac, K. Lipowski, J. Ullah, S. Fields, J.H. Kramer, J. Merrilees, J. Neuhaus, M. M. Mesulam, B.L. Miller, Memantine in patients with frontotemporal lobar degeneration: a multicentre, randomised, double-blind, placebo-controlled trial, *Lancet Neurol.* 12 (2013) 149–156, [https://doi.org/10.1016/S1474-4422\(12\)70320-4](https://doi.org/10.1016/S1474-4422(12)70320-4).
- [15] R.A. Hansen, G. Gartlehner, A.P. Webb, L.C. Morgan, C.G. Moore, D.E. Jonas, Efficacy and safety of donepezil, galantamine, and rivastigmine for the treatment of Alzheimer's disease: a systematic review and meta-analysis, *Clin. Interv. Aging* 3 (2008) 211–225, <http://www.ncbi.nlm.nih.gov/pubmed/18686744>.
- [16] G. Riedel, Glutamate receptor function in learning and memory, *Behav. Brain Res.* 140 (2003) 1–47, [https://doi.org/10.1016/S0166-4328\(02\)00272-3](https://doi.org/10.1016/S0166-4328(02)00272-3).
- [17] S.J. Martin, P.D. Grimwood, R.G.M. Morris, Synaptic plasticity and memory: an evaluation of the hypothesis, *Annu. Rev. Neurosci.* 23 (2000) 649–711, <https://doi.org/10.1146/annurev.neuro.23.1.649>.
- [18] R.G.M. Morris, E.I. Moser, G. Riedel, S.J. Martin, J. Sandin, M. Day, C. O'Carroll, Elements of a neurobiological theory of the hippocampus: the role of activity-dependent synaptic plasticity in memory, *Philos. Trans. R. Soc. Lond. Ser. B Biol. Sci.* 358 (2003) 773–786, <https://doi.org/10.1098/rstb.2002.1264>.
- [19] T. Takeuchi, A.J. Duszkievicz, R.G.M. Morris, The synaptic plasticity and memory hypothesis: encoding, storage and persistence, *Philos. Trans. R. Soc. B Biol. Sci.* 369 (2014) 20130288, <https://doi.org/10.1098/rstb.2013.0288>.
- [20] A. Leuzy, E.R. Zimmer, J. Dubois, J. Pruessner, C. Cooperman, J.-P. Soucy, A. Kostikov, E. Schirmachner, R. Désautels, S. Gauthier, P. Rosa-Neto, In vivo characterization of metabotropic glutamate receptor type 5 abnormalities in behavioral variant FTD, *Brain Struct. Funct.* 221 (2016) 1387–1402, <https://doi.org/10.1007/s00429-014-0978-3>.
- [21] D.M. Bowen, A.W. Procter, D.M.A. Mann, J.S. Snowden, M.M. Esiri, D. Neary, P. T. Francis, Imbalance of a serotonergic system in frontotemporal dementia: implication for pharmacotherapy, *Psychopharmacology* 196 (2008) 603–610, <https://doi.org/10.1007/s00213-007-0992-8>.
- [22] C.C. Rudy, H.C. Hunsberger, D.S. Weitzner, M.N. Reed, The role of the tripartite glutamatergic synapse in the pathophysiology of Alzheimer's disease, *Aging Dis.* 6 (2015) 131, <https://doi.org/10.14336/AD.2014.0423>.
- [23] T. Storck, S. Schulte, K. Hofmann, W. Stoffel, Structure, expression, and functional analysis of a Na⁺-dependent glutamate/aspartate transporter from rat brain, *Proc. Natl. Acad. Sci.* 89 (1992) 10955–10959, <https://doi.org/10.1073/pnas.89.22.10955>.
- [24] G. Pines, N.C. Danbolt, M. Björås, Y. Zhang, A. Bendahan, L. Eide, H. Koepsell, J. Storm-Mathisen, E. Seeberg, B.I. Kanner, Cloning and expression of a rat brain L-glutamate transporter, *Nature* 360 (1992) 464–467, <https://doi.org/10.1038/360464a0>.
- [25] S. Mahmoud, M. Gharagozloo, C. Simard, D. Gris, Astrocytes maintain glutamate homeostasis in the CNS by controlling the balance between glutamate uptake and release, *Cells* 8 (2019) 184, <https://doi.org/10.3390/cells8020184>.
- [26] K.P. Lehre, N.C. Danbolt, The number of glutamate transporter subtype molecules at glutamatergic synapses: chemical and stereological quantification in young adult rat brain, *J. Neurosci.* 18 (1998) 8751–8757, <https://doi.org/10.1523/JNEUROSCI.18-21-08751.1998>.
- [27] M. Haris, K. Nath, K. Cai, A. Singh, R. Crescenzi, F. Kogan, G. Verma, S. Reddy, H. Hariharan, E.R. Melhem, R. Reddy, Imaging of glutamate neurotransmitter alterations in Alzheimer's disease, *NMR Biomed.* 26 (2013) 386–391, <https://doi.org/10.1002/nbm.2875>.
- [28] P.T. Francis, N.R. Sims, A.W. Procter, D.M. Bowen, Cortical pyramidal neuron loss may cause glutamatergic hypoactivity and cognitive impairment in Alzheimer's disease: investigative and therapeutic perspectives, *J. Neurochem.* 60 (1993) 1589–1604, <https://doi.org/10.1111/j.1471-4159.1993.tb13381.x>.
- [29] T. Revett, G. Baker, J. Jhamandas, S. Kar, Glutamate system, amyloid β peptides and tau protein: functional interrelationships and relevance to Alzheimer disease pathology, *J. Psychiatry Neurosci.* 38 (2013) 6–23, <https://doi.org/10.1503/jpn.110190>.
- [30] A. Kashani, È. Lepicard, O. Poirel, C. Videau, J.P. David, C. Fallet-Bianco, A. Simon, A. Delacourte, B. Giros, J. Epelbaum, C. Betancur, S. El Mestikawy, Loss of VGLUT1 and VGLUT2 in the prefrontal cortex is correlated with cognitive decline in Alzheimer disease, *Neurobiol. Aging* 29 (2008) 1619–1630, <https://doi.org/10.1016/j.neurobiolaging.2007.04.010>.
- [31] P. Sokoloff, L. Leriche, J. Diaz, J. Louvel, R. Pumain, Direct and indirect interactions of the dopamine D3 receptor with glutamate pathways: implications for the treatment of schizophrenia, *Naunyn-Schmiedeberg Arch. Pharmacol.* 386 (2013) 107–124, <https://doi.org/10.1007/s00210-012-0797-0>.
- [32] E. Masliah, L. Hansen, M. Alford, R. DeTeresa, M. Mallory, Deficient glutamate transport is associated with neurodegeneration in Alzheimer's disease, *Ann. Neurol.* 40 (1996) 759–766, <https://doi.org/10.1002/ana.410400512>.
- [33] H.A. Scott, F.M. Gebhardt, A.D. Mitrovic, R.J. Vandenberg, P.R. Dodd, Glutamate transporter variants reduce glutamate uptake in Alzheimer's disease, *Neurobiol. Aging* 32 (2011) e1–e53, <https://doi.org/10.1016/j.neurobiolaging.2010.03.008>.
- [34] L. Emilsson, P. Saetre, E. Jazin, Alzheimer's disease: mRNA expression profiles of multiple patients show alterations of genes involved with calcium signaling, *Neurobiol. Dis.* 21 (2006) 618–625, <https://doi.org/10.1016/j.nbd.2005.09.004>.
- [35] B. Winblad, R.W. Jones, Y. Wirth, A. Stöfller, H.J. Möbius, Memantine in moderate to severe Alzheimer's disease: a meta-analysis of randomised clinical trials, *Dement. Geriatr. Cogn. Disord.* 24 (2007) 20–27, <https://doi.org/10.1159/000102568>.
- [36] S. Sokolov, K.M. Henkins, T. Bilousova, B. Gonzalez, H.V. Vinters, C.A. Miller, L. Cornwell, W.W. Poon, K.H. Gyls, Pre-synaptic C-terminal truncated tau is released from cortical synapses in Alzheimer's disease, *J. Neurochem.* 133 (2015) 368–379, <https://doi.org/10.1111/jnc.12991>.
- [37] N. Sahara, M. Murayama, M. Higuchi, T. Suhara, A. Takashima, Biochemical distribution of tau protein in synaptosomal fraction of transgenic mice expressing human P301L tau, *Front. Neurol.* 5 (2014) 26, <https://doi.org/10.3389/fneur.2014.00026>.
- [38] L. Zhou, J. McInnes, K. Wierda, M. Holt, A.G. Herrmann, R.J. Jackson, Y.-C. Wang, J. Swerts, J. Beyens, K. Miskiewicz, S. Vilain, I. Dewachter, D. Moechars, B. De Strooper, T.L. Spire-Jones, J. De Wit, P. Verstreken, Tau association with synaptic vesicles causes presynaptic dysfunction, *Nat. Commun.* 8 (2017) 15295, <https://doi.org/10.1038/ncomms15295>.
- [39] N. Lemke, V. Melis, L. Dilyara, M. Mandy, B. Neumann, C. Harrington, G. Riedel, C. Wischik, F. Theuring, K. Schwab, Differential compartmental processing and phosphorylation of pathogenic human tau and native mouse tau in the line 66 model of frontotemporal dementia, *J. Biol. Chem.* 296 (2020) 18508–18523, <https://doi.org/10.1074/jbcRA120.014890>.
- [40] H.C. Hunsberger, C.C. Rudy, S.R. Batten, G.A. Gerhardt, M.N. Reed, P301L tau expression affects glutamate release and clearance in the hippocampal trisynaptic pathway, *J. Neurochem.* 132 (2015) 169–182, <https://doi.org/10.1111/jnc.12967>.
- [41] D.V. Dabir, Impaired glutamate transport in a mouse model of tau pathology in astrocytes, *J. Neurosci.* 26 (2006) 644–654, <https://doi.org/10.1523/JNEUROSCI.3861-05.2006>.
- [42] H.C. Hunsberger, D.S. Weitzner, C.C. Rudy, J.E. Hickman, E.M. Libell, R.R. Speer, G.A. Gerhardt, M.N. Reed, Riluzole rescues glutamate alterations, cognitive deficits, and tau pathology associated with P301L tau expression, *J. Neurochem.* 135 (2015) 381–394, <https://doi.org/10.1111/jnc.13230>.
- [43] H.C. Hunsberger, J.E. Hickman, M.N. Reed, Riluzole rescues alterations in rapid glutamate transients in the hippocampus of rTg4510 mice, *Metab. Brain Dis.* 31 (2016) 711–715, <https://doi.org/10.1007/s11011-015-9783-9>.
- [44] K. Yamada, J.K. Holth, F. Liao, F.R. Stewart, T.E. Mahan, H. Jiang, J.R. Cirrito, T. K. Patel, K. Hochgräfe, E.-M. Mandelkow, D.M. Holtzman, Neuronal activity regulates extracellular tau in vivo, *J. Exp. Med.* 211 (2014) 387–393, <https://doi.org/10.1084/jem.20131685>.
- [45] F. Florenzano, C. Veronica, G. Ciasca, M.T. Ciotti, A. Pittaluga, G. Olivero, M. Feligioni, F. Iannuzzi, V. Latina, M.F. Maria Sciacca, A. Sinopoli, D. Milardi, G. Pappalardo, D.S. Marco, M. Papi, A. Atlante, A. Bobba, A. Borreca, P. Calissano, G. Amadoro, Extracellular truncated tau causes early presynaptic dysfunction associated with Alzheimer's disease and other tauopathies, *Oncotarget* 8 (2017) 64745–64778, <https://doi.org/10.18632/oncotarget.17371>.
- [46] V. Melis, C. Zabke, K. Stamer, M. Magbagbeolu, K. Schwab, P. Marschall, R.W. Veh, S. Bachmann, S. Deiana, P.-H. Moreau, K. Davidson, K.A. Harrington, J.E. Rickard, D. Horsley, R. Garman, M. Mazurkiewicz, G. Niewiadomska, C.M. Wischik, C. R. Harrington, G. Riedel, F. Theuring, Different pathways of molecular pathophysiology underlie cognitive and motor tauopathy phenotypes in transgenic models for Alzheimer's disease and frontotemporal lobar degeneration, *Cell. Mol. Life Sci.* 72 (2015) 2199–2222, <https://doi.org/10.1007/s00018-014-1804-z>.
- [47] H. Braak, E. Braak, Neuropathological staging of Alzheimer-related changes, *Acta Neuropathol.* 82 (1991) 239–259, <https://doi.org/10.1007/BF00308809>.
- [48] V. Melis, M. Magbagbeolu, J.E. Rickard, D. Horsley, K. Davidson, K.A. Harrington, K. Goatman, E.A. Goatman, S. Deiana, S.P. Close, C. Zabke, K. Stamer, S. Dietze, K. Schwab, J.M.D. Storey, C.R. Harrington, C.M. Wischik, F. Theuring, G. Riedel, Effects of oxidized and reduced forms of methylthioninium in two transgenic mouse tauopathy models, *Behav. Pharmacol.* 26 (2015) 353–368, <https://doi.org/10.1097/FBP.0000000000000133>.
- [49] B.O. Schelter, H. Shiells, T.C. Baddeley, C.M. Rubino, H. Ganesan, J. Hammel, V. Vuksanovic, R.T. Staff, A.D. Murray, L. Bracoud, G. Riedel, S. Gauthier, J. Jia, P. Bentham, K. Kook, J.M.D. Storey, C.R. Harrington, C.M. Wischik, Concentration-

- dependent activity of hydromethylthionine on cognitive decline and brain atrophy in mild to moderate Alzheimer's disease, *J. Alzheimers Dis.* (2019), <https://doi.org/10.3233/JAD-190772>.
- [50] H. Shiells, B.O. Schelter, P. Bentham, T.C. Baddeley, C.M. Rubino, H. Ganesan, J. Hammel, V. Vuksanovic, R.T. Staff, A.D. Murray, L. Bracoud, D.J. Wischik, G. Riedel, S. Gauthier, J. Jia, H.J. Moebius, J. Hardlund, C.M. Kipps, K. Kook, J.M. D. Storey, C.R. Harrington, C.M. Wischik, Concentration-dependent activity of hydromethylthionine on clinical decline and brain atrophy in a randomized controlled trial in behavioral variant frontotemporal dementia, *J. Alzheimers Dis.* 75 (2020) 501–519, <https://doi.org/10.3233/JAD-191173>.
- [51] K.J. Smillie, G.J.O. Evans, M.A. Cousin, Developmental change in the calcium sensor for synaptic vesicle endocytosis in central nerve terminals, *J. Neurochem.* 94 (2005) 452–458, <https://doi.org/10.1111/j.1471-4159.2005.03213.x>.
- [52] C.Y. Chang, C.F. Hung, S.K. Huang, J.R. Kuo, S.J. Wang, Amiodarone reduces depolarization-evoked glutamate release from hippocampal synaptosomes, *J. Pharmacol. Sci.* 133 (2017) 168–175, <https://doi.org/10.1016/j.jpsh.2017.02.014>.
- [53] N. Percie du Sert, V. Hurst, A. Ahluwalia, S. Alam, M. Avey, M. Baker, W. Browne, A. Clark, I. Cuthill, U. Dirnagl, M. Emerson, P. Garner, S. Holgate, D. Howells, N. Karp, K. Lidster, C. MacCallum, M. Macleod, O. Petersen, F. Rawle, P. Reynolds, K. Rooney, E. Sena, S. Silberberg, T. Steckler, H. Würbel, The ARRIVE guidelines 2019: updated guidelines for reporting animal research, *BioRxiv* (2019), <https://doi.org/10.1101/703181>.
- [54] T.C. Baddeley, J. McCaffrey, J.M.D. Storey, J.K.S. Cheung, V. Melis, D. Horsley, C. R. Harrington, C.M. Wischik, Complex disposition of methylthioninium redox forms determines efficacy in tau aggregation inhibitor therapy for Alzheimer's disease, *J. Pharmacol. Exp. Ther.* 352 (2015) 110–118, <https://doi.org/10.1124/jpet.114.219352>.
- [55] Y.K. Al-Hilaly, S.J. Pollack, J.E. Rickard, M. Simpson, A.-C. Raulin, T. Baddeley, P. Schellenberger, J.M.D. Storey, C.R. Harrington, C.M. Wischik, L.C. Serpell, Cysteine-independent inhibition of Alzheimer's disease-like paired helical filament assembly by leuco-methylthioninium (LMT), *J. Mol. Biol.* 430 (2018) 4119–4131, <https://doi.org/10.1016/j.jmb.2018.08.010>.
- [56] C.R. Harrington, J.M.D. Storey, S. Clunas, K.A. Harrington, D. Horsley, A. Ishaq, S. J. Kemp, C.P. Larch, C. Marshall, S.L. Nicoll, J.E. Rickard, M. Simpson, J.P. Sinclair, L.J. Storey, C.M. Wischik, Cellular models of aggregation-dependent template-directed proteolysis to characterize tau aggregation inhibitors for treatment of Alzheimer disease, *J. Biol. Chem.* 290 (2015) 10862–10875, <https://doi.org/10.1074/jbc.M114.616029>.
- [57] A.W.P. Fitzpatrick, B. Falcon, S. He, A.G. Murzin, G. Murshudov, H.J. Garringer, R. A. Crowther, B. Ghetti, M. Goedert, S.H.W. Scheres, Cryo-EM structures of tau filaments from Alzheimer's disease, *Nature* 547 (7662) (2017) 185–190, <https://doi.org/10.1038/nature23002>.
- [58] B. Falcon, W. Zhang, A.G. Murzin, G. Murshudov, H.J. Garringer, R. Vidal, R. A. Crowther, B. Ghetti, S.H.W. Scheres, M. Goedert, Structures of filaments from Pick's disease reveal a novel tau protein fold, *Nature* 561 (2018) 137–140, <https://doi.org/10.1038/s41586-018-0454-y>.
- [59] Y.K. Al-Hilaly, B.E. Foster, L. Biasetti, L. Lutter, S.J. Pollack, J.E. Rickard, J.M. D. Storey, C.R. Harrington, W. Xue, C.M. Wischik, L.C. Serpell, Tau (297–391) forms filaments that structurally mimic the core of paired helical filaments in Alzheimer's disease brain, *FEBS Lett.* 594 (2020) 944–950, <https://doi.org/10.1002/1873-3468.13675>.
- [60] S. Dujardin, C. Commins, A. Lathuiliere, P. Beerepoot, A.R. Fernandes, T. V. Kamath, M.B. De Los Santos, N. Wlickstein, D.L. Corjuc, B.T. Corjuc, P.M. Dooley, A. Viode, D.H. Oakley, B.D. Moore, K. Mullin, D. Jean-Gilles, R. Clark, K. Atchison, R. Moore, L.B. Chibnik, R.E. Tanzi, M.P. Frosch, A. Serrano-Pozo, F. Elwood, J. A. Steen, M.E. Kennedy, B.T. Hyman, Tau molecular diversity contributes to clinical heterogeneity in Alzheimer's disease, *Nat. Med.* 26 (2020) 1256–1263, <https://doi.org/10.1038/s41591-020-0938-9>.
- [61] G. Riedel, J. Klein, G. Niewiadomska, K. Kondak, K. Schwab, D. Lauer, M. Magbagbeolu, M. Steczkowska, M. Zdrozny, M. Wydrych, A. Cranston, V. Melis, R.X. Santos, F. Theuring, C.R. Harrington, C.M. Wischik, Mechanisms of anticholinesterase interference with tau aggregation inhibitor activity in a tau-transgenic mouse model, *Curr. Alzheimer Res.* 17 (2020) 285–296, <https://doi.org/10.2174/1567205017666200224120926>.
- [62] A. Kremer, H. Maurin, D. Demedis, H. Devijver, P. Borghgraef, F. Van Leuven, Early improved and late defective cognition is reflected by dendritic spines in tau. P301L mice, *J. Neurosci.* 31 (2011) 18036–18047, <https://doi.org/10.1523/JNEUROSCI.4859-11.2011>.
- [63] F. Mazzo, I. Butnaru, O. Grubisha, E. Ficulle, H. Sanger, G. Fitzgerald, F. Pan, F. Pasqui, T. Murray, J. Monn, X. Li, M. Hutton, S. Bose, G. Schiavo, E. Sher, Metabotropic glutamate receptors modulate exocytotic tau release and propagation, *J. Pharmacol. Exp. Therapeut* 2 (2022) 117–128, <https://doi.org/10.1124/jpet.122.001307>.
- [64] I. Bezprozvanny, M.P. Mattson, Neuronal calcium mishandling and the pathogenesis of Alzheimer's disease, *Trends Neurosci.* 31 (2008) 454–463, <https://doi.org/10.1016/j.tins.2008.06.005>.
- [65] P. Marambaud, U. Dreses-Werringloer, V. Vingtdoux, Calcium signaling in neurodegeneration, *Mol. Neurodegener.* 4 (2009) 20, <https://doi.org/10.1186/1750-1326-4-20>.
- [66] A.C. Dolphin, A. Lee, Presynaptic calcium channels: specialized control of synaptic neurotransmitter release, *Nat. Rev. Neurosci.* 21 (2020) 213–229, <https://doi.org/10.1038/s41583-020-0278-2>.
- [67] A. Scimemi, J.S. Diamond, The number and organization of Ca²⁺ channels in the active zone shapes neurotransmitter release from Schaffer collateral synapses, *J. Neurosci.* 32 (2012) 18157–18176, <https://doi.org/10.1523/JNEUROSCI.3827-12.2012>.
- [68] P.E. Castillo, Presynaptic LTP and LTD of excitatory and inhibitory synapses, *Cold Spring Harb. Perspect. Biol.* 4 (2012) a005728, <https://doi.org/10.1101/cshperspect.a005728>.
- [69] M.S. Ahmed, S.A. Siegelbaum, Recruitment of N-type Ca²⁺ channels during LTP enhances low release efficacy of hippocampal CA1 perforant path synapses, *Neuron* 63 (2009) 372–385, <https://doi.org/10.1016/j.neuron.2009.07.013>.
- [70] C. Chen, W.G. Regehr, The mechanism of cAMP-mediated enhancement at a cerebellar synapse, *J. Neurosci.* 17 (1997) 8687–8694, <https://doi.org/10.1523/JNEUROSCI.17-22-08687.1997>.
- [71] K. Schwab, D. Lauer, M. Magbagbeolu, F. Theuring, A. Gasiorowska, M. Zdrozny, C.R. Harrington, C.M. Wischik, G. Niewiadomska, G. Riedel, Hydromethylthionine rescues synaptic SNARE proteins in a mouse model of tauopathies: interference by cholinesterase inhibitors, *Brain Res. Bull.* 212 (2024) 110955, <https://doi.org/10.1016/j.brainresbull.2024.110955>.
- [72] J.W. Johnson, S.E. Kotermanski, Mechanism of action of memantine, *Curr. Opin. Pharmacol.* 6 (2006) 61–67, <https://doi.org/10.1016/j.coph.2005.09.007>.
- [73] N.O. Dalby, C. Volbracht, L. Helboe, P.H. Larsen, H.S. Jensen, J. Egebjerg, A. B. Elvang, Altered function of hippocampal CA1 pyramidal neurons in the rTg4510 mouse model of tauopathy, *J. Alzheimers Dis.* 40 (2014) 429–442, <https://doi.org/10.3233/JAD-131358>.
- [74] M. Shimojo, H. Takuwa, Y. Takado, M. Tokunaga, S. Tsukamoto, K. Minatohara, M. Ono, C. Seki, J. Maeda, T. Urushihata, T. Minamihisamatsu, I. Aoki, K. Kawamura, M.-R. Zhang, T. Suhara, N. Sahara, M. Higuchi, Selective disruption of inhibitory synapses leading to neuronal hyperexcitability at an early stage of tau pathology in a mouse model, *J. Neurosci.* 40 (2020) 3491–3501, <https://doi.org/10.1523/JNEUROSCI.2880-19.2020>.
- [75] B.A. Warmus, D.R. Sekar, E. McCutchen, G.D. Schellenberg, R.C. Roberts, L. L. McMahon, E.D. Roberson, Tau-mediated NMDA receptor impairment underlies dysfunction of a selectively vulnerable network in a mouse model of frontotemporal dementia, *J. Neurosci.* 34 (2014) 16482–16495, <https://doi.org/10.1523/JNEUROSCI.3418-14.2014>.
- [76] E. Hill, T.K. Karikari, K.G. Moffat, M.J.E. Richardson, M.J. Wall, Introduction of tau oligomers into cortical neurons alters action potential dynamics and disrupts synaptic transmission and plasticity, *eNeuro* 6 (2019), <https://doi.org/10.1523/ENEURO.0166-19.2019>.
- [77] T. Ondrejcek, I. Klyubin, G.T. Corbett, G. Fraser, W. Hong, A.J. Mably, M. Gardener, J. Hammersley, M.S. Perkinson, A. Billinton, D.M. Walsh, M. J. Rowan, Cellular prion protein mediates the disruption of hippocampal synaptic plasticity by soluble tau in vivo, *J. Neurosci.* 38 (2018) 10595–10606, <https://doi.org/10.1523/JNEUROSCI.1700-18.2018>.
- [78] F. Tamagnini, D.A. Walsh, J.T. Brown, M.K. Bondulich, D.P. Hanger, A.D. Randall, Hippocampal neurophysiology is modified by a disease-associated C-terminal fragment of tau protein, *Neurobiol. Aging* 60 (2017) 44–56, <https://doi.org/10.1016/j.neurobiolaging.2017.07.005>.
- [79] S. Mondragón-Rodríguez, A. Salas-Gallardo, P. González-Pereyra, M. Macías, B. Ordaz, F. Peña-Ortega, A. Aguilar-Vázquez, E. Orta-Salazar, S. Díaz-Cintra, G. Perry, S. Williams, Phosphorylation of tau protein correlates with changes in hippocampal theta oscillations and reduces hippocampal excitability in Alzheimer's model, *J. Biol. Chem.* 293 (2018) 8462–8472, <https://doi.org/10.1074/jbc.RA117.001187>.
- [80] P.D. Sohn, C.T.-L. Huang, R. Yan, L. Fan, T.E. Tracy, C.M. Camargo, K. M. Montgomery, T. Arhar, S.-A. Mok, R. Freilich, J. Baik, M. He, S. Gong, E. D. Roberson, C.M. Karch, J.E. Gestwicki, K. Xu, K.S. Kosik, L. Gan, Pathogenic tau impairs axon initial segment plasticity and excitability homeostasis, *Neuron* 104 (2019) 458–470.e5, <https://doi.org/10.1016/j.neuron.2019.08.008>.
- [81] L.H. Nilsen, C. Rae, L.M. Ittner, J. Götz, U. Sonnewald, Glutamate metabolism is impaired in transgenic mice with tau hyperphosphorylation, *J. Cereb. Blood Flow Metab.* 33 (2013) 684–691, <https://doi.org/10.1038/jcbfm.2012.212>.
- [82] B. Bolon, M.T. Butt, *Fundamental Neuropathology for Pathologists and Toxicologists*, John Wiley & Sons, Inc, Hoboken, NJ, USA, 2011, <https://doi.org/10.1002/9780470939956>.
- [83] W. Löscher, G. Böhme, F. Müller, S. Pagliusi, Improved method for isolating synaptosomes from 11 regions of one rat brain: electron microscopic and biochemical characterization and use in the study of drug effects on nerve terminal γ-aminobutyric acid in vivo, *J. Neurochem.* 45 (1985) 879–889, <https://doi.org/10.1111/j.1471-4159.1985.tb04076.x>.